Brain Imaging and Behavior
DOI 10.1007/s11682-017-9769-9

ORIGINAL RESEARCH

White matter fiber bundle lengths are shorter in cART naive HIV: an analysis of quantitative diffusion tractography in South Africa

Jodi M. Heaps-Woodruff[1] · John Joska[2] · Ryan Cabeen[3] · Laurie M. Baker[1] · Lauren E. Salminen[4] · Jacqueline Hoare[2] · David H. Laidlaw[3,5] · Rachel Wamser-Nanney[6] · Chun-Zi Peng[1] · Susan Engelbrecht[7] · Soraya Seedat[7] · Dan J. Stein[8] · Robert H. Paul[1]

Abstract This study examines white matter microstructure using quantitative tractography diffusion magnetic resonance imaging (qtdMRI) in HIV+ individuals from South Africa who were naïve or early in the initiation of antiretroviral therapy. Fiber bundle length (FBL) metrics, generated from qtdMRI, for whole brain and six white matter tracts of interest (TOI) were assessed for 135 HIV+ and 21 HIV− individuals. The association between FBL metrics, measures of disease burden, and neuropsychological performance were also investigated. Results indicate significantly reduced sum of whole brain fiber bundle lengths (FBL, $p < 0.001$), but not average whole brain FBL in the HIV+ group compared to the HIV− controls. The HIV+ group exhibited significantly shorter sum of FBL in all six TOIs examined: the anterior thalamic radiation, cingulum bundle, inferior and superior longitudinal fasciculi, inferior frontal occipital fasciculus, and the uncinate fasciculus. Additionally, average FBLs were significantly shorter select TOIs including the inferior longitudinal fasciculus, cingulum bundle, and the anterior thalamic radiation. Shorter whole brain FBL sum metrics were associated with poorer neuropsychological performance, but were not associated with markers of disease burden. Taken together these findings suggest HIV affects white matter architecture primarily through reductions in white matter fiber numbers and, to a lesser degree, the shortening of fibers along a bundle path.

Keywords HIV · Quantitative tractography · Diffusion tensor imaging · Cognition

Introduction

HIV-positive (HIV+) individuals, even when on effective treatment for HIV, continue to experience chronic symptoms in multiple organ systems, including the brain (Nath 2015). Many studies have shown that HIV impacts both gray and white matter in the brain, resulting in abnormalities in neuroimaging markers of brain integrity and neurocognitive

Electronic supplementary material The online version of this article (https://doi.org/10.1007/s11682-017-9769-9) contains supplementary material, which is available to authorized users.

✉ Jodi M. Heaps-Woodruff
heapsj@umsl.edu

[1] Missouri Institute of Mental Health, University of Missouri, St. Louis, MO, USA

[2] Department of Psychiatry and Mental Health, University of Cape Town, Cape Town, South Africa

[3] Laboratory of Neuro Imaging, Mark and Mary Stevens Neuroimaging and Informatics Institute, Keck School of Medicine of USC, University of Southern California, Los Angeles, CA, USA

[4] Mark and Mary Stevens Neuroimaging and Informatics Institute, Imaging Genetics Center, University of Southern California, Los Angeles, CA, USA

[5] Department of Computer Science, Brown University, Providence, RI, USA

[6] Department of Psychology, University of Missouri-St. Louis, St. Louis, MO, USA

[7] Division of Medical Virology, Stellenbosch University and National Health Laboratory Services (NHLS), Cape Town, South Africa

[8] MRC Unit on Risk & Resilience in Mental Disorders, Department of Psychiatry, University of Stellenbosch, Stellenbosch, South Africa

Published online: 06 November 2017

impairment (Ances and Hammoud 2014). Clinical studies reveal that the deleterious impact of HIV on brain structure and function is independent of viral clade (Buch et al. 2016), including clade C (HIV-C) which is dominant in South Africa ((de Almeida et al. 2013); (Paul et al. 2014); (Hoare et al. 2011; Joska et al. 2010, 2011, 2012)).

Neuroimaging outcomes in HIV-C correspond with the extant literature in HIV clade B (HIV-B), indicating smaller brain volumes (Heaps et al. 2012; Ortega et al. 2013) in treatment naïve HIV+ individuals compared to uninfected controls. Smaller volumes in gray and white matter, and the thalamus correlated with worse performance on brief measures of cognitive functioning such as the international HIV dementia screen and a four item neuropsychological battery (e.g. NPZ-4) (Heaps et al. 2012; Ortega et al. 2013). Additionally, these smaller brain volumes correspond to measures of disease burden including lower CD4 cell counts and greater HIV viral load (Heaps et al. 2012; Ortega et al. 2013). In general, HIV studies of white matter using diffusion tensor imaging (DTI) show lower fractional anisotropy and increased diffusion in HIV+ individuals compared to controls (for review see Masters and Ances 2014; Thompson and Jahanshad 2015). These changes may reflect demyelination and axonal degradation (Alexander et al. 2011), are evident in early infection (Ragin et al. 2015), in cART treated populations (Wright et al. 2012), and may be intensified with age (Seider et al. 2016). White matter microstructure has also been examined in pediatric and adult HIV+ individuals in South Africa, with abnormal DTI scalar metrics evident in HIV+ individuals independent of the genetic polymorphism in the viral Tat protein common in clade C disease (Paul et al. 2017). Furthermore, studies have reported HIV-associated abnormal white matter microstructure in individuals with the APOE4 genotype (Hoare et al. 2013), poor prospective memory (Hoare et al. 2012), apathy (Hoare et al. 2010), and children receiving antiretroviral therapy (ART;(Hoare et al. 2015). Most recent studies in South Africa have found disruptions of structural brain networks in HIV+ individuals compared to healthy participants (Baker et al. 2017).

One limitation of structural imaging and traditional approaches to DTI metrics is the lack of detail about the organization and microstructure of white matter tracts due to data averaging at the voxel or regional level. Additionally, single tensor models only capture the directionality of tracts along the primary eigenvector, although it is possible to use multi-tensor models. Quantitative tractography diffusion magnetic resonance imaging (qtdMRI) is an alternative diffusion processing technique with high sensitivity to changes in the microstructure of white matter fibers. Fiber bundle lengths (FBLs) are computed using scalar DTI metrics, such as FA, in concert with tractography methods to delineate bundles of nerve fibers. A number of metrics are available, such as average FBL weighted by scalar DTI metrics, or a summation of FBL in the whole brain or in a given white matter tract. The metrics provide information about the underlying microstructure of white matter in better detail than previous methods. Additional information about the length, volume, and organization of fibers within a tract of interest (TOI) can be obtained using qdtMRI (Correia et al. 2008)). Previous investigations have demonstrated the clinical relevance of these metrics across several conditions (Baker et al. 2014); (Bolzenius et al. 2013); (Correia et al. 2008), but limited work has been conducted in HIV. Tate et al. utilized an early version of qtdMRI based on single fiber modeling to examine white matter integrity in 23 treatment-naive individuals with HIV-B compared to 20 HIV− controls. Results of the preliminary study revealed reduced tractography FA among HIV+ individuals at a global level, and a significant correlation between the imaging metric and worse cognitive performance. To date, no studies have examined white matter integrity in HIV-C using qtdMRI, and prior work has not utilized multi-fiber modeling which reduces limitations of single-tensor models such as partial volume effects or crossing fiber effects of prior tractography methods (Cabeen et al. 2016).

The purpose of this study was to examine differences in qtdMRI FBL in both whole brain and six TOI between HIV− and HIV+ individuals with HIV-C. The TOIs were selected to allow comparison to prior DTI studies in HIV (Hoare et al. 2012; Tate et al. 2010) and other FBL studies (Baker et al. 2016; Behrman-Lay et al. 2015; Bolzenius et al. 2015). We selected average FBL and summed FBL metrics in both whole brain and selected tracts. The metrics were selected as they reflect complementary information about the underlying architecture of the white matter fibers that cannot be determined with standard DTI metrics such as FA and MD. Additionally, we chose long-range fiber bundles that connect the frontal lobe to the temporal, parietal, and occipital lobes. Average FBL reflects the average length of all the fibers within a given tract, or throughout the whole brain whereas summed FBL reflects the summation of all FBL within a tract or throughout the brain. In group comparisons, if average FBL is reduced in one group compared to the other this suggests an overall shortening of fibers. If summed FBL is reduced then it may reflect an overall loss of fibers, a change in the underlying architecture of the fiber, or reduction in fiber density. If they are both reduced, then this suggests both a loss of fibers as well as a shortening of fibers. We anticipated that HIV+ individuals would have shorter average FBL and summed FBL compared to HIV− individuals. We further examined the relationships between FBL metrics, markers of HIV disease burden (i.e., duration of infection, viral load, current CD4 cell count), and neuropsychological performance. We expected that FBL metrics would

correlate with clinical laboratory variables and cognitive performance.

Methods

Participants

A total of 135 HIV+ individuals and 21 HIV− individuals completed neuroimaging at the University of Cape Town (UCT) in South Africa. All individuals consented to the protocol as approved by the ethics committee at UCT. In order to be included in the study, individuals were required to be between the ages of 18–45, speak Xhosa as their primary language, and have completed a minimum of five years of formal education. Additional inclusion criteria for the HIV+ group included: (1) Documented HIV serostatus by Elisa and confirmed by Western Blot; and (2) Naïve to (ART) or be within the first 30 days of ART initiation. Criteria for exclusion from the study for all participants were as follows: (1) Any current or past major DSM-IV Axis I psychiatric condition that could significantly affect cognitive status (e.g., schizophrenia or bipolar disorder); (2) Confounding neurological disorders including multiple sclerosis and other CNS conditions; (3) Head injury with loss of consciousness greater than 30 min; (4) Clinical evidence of opportunistic CNS infections (e.g., toxoplasmosis, progressive multifocal leukoencephalopathy, neoplasms); (5) Current substance use or alcohol use disorder as determined by a structured interview; and (6) Visual evidence of brain injury (e.g. stroke) on neuroimaging.

Recruitment of HIV+ participants occurred at community ART clinics in Cape Town, South Africa. Interested participants consented to participate and then completed a detailed medical and demographic survey. Study participation was voluntary and individuals were free to withdraw from the study at any point. Participants were compensated for assessments and transportation was provided for each study visit. HIV− participants were recruited from regional Voluntary Counseling and Testing Clinics in Cape Town, South Africa and were required to have laboratory-confirmed seronegative status. Recruitment from these clinics was intended to minimize differences in key demographic variables between the two groups (e.g., language, education, socioeconomic status). The study was approved by the Human Ethics Committee of the University of Cape Town, South Africa and the University of Missouri-St. Louis Institutional Review Board.

HIV viral load, CD4 + cell counts, and duration of infection

Blood samples were collected within 1 week of the MRI acquisition. RNA was isolated from patient samples using the Abbott RealTime HIV-1 amplification reagent kit, according to the manufacturer's instructions. Viral load was calculated using the Abbott m2000sp and the Abbott m2000rt analysers (Abbott laboratories, Abbott Park, Illinois, USA). CD4 + cell count was analyzed from blood samples and completed on the FACSCalibur flow cytometer in conjunction with the MultiSET V1.1.2 software (BD Biosciences, San Jose, CA, USA). Date of HIV diagnosis was available from clinic records for the majority ($n = 111$) of HIV+ individuals.

PCR amplification and sequencing of the tat exon 1 region

The tat exon 1 region was amplified (HXB2 position 5831–6045) by polymerase chain reaction (PCR) using the Promega GoTaq Flexi Kit (Promega, Madison, WI) according to manufacturer's instructions. Details have been described previously (Paul et al. 2014). In brief, The PCR products were purified, sequenced and analyzed. Nucleotide sequences were used to translate info into amino acid sequences. HIV subtypes were determined to confirm HIV-C clade status for study inclusion.

Neuroimaging acquisition

Imaging acquisition took place using a head-only Magnetom Allegra 3 T MRI scanning system (Siemens Medical Solutions, Erlangen, Germany) with a 4-channel phased-array head coil. A head stabilizer was used to minimize movement. Head placement was confirmed by a preliminary scout scan composed of three orthogonal planes. A T1-weighted magnetization-prepared rapid acquisition gradient echo (MP-RAGE) sequence was acquired using a T1-weighted three dimensional magnetization-prepared rapid acquisition gradient echo (MPRAGE) sequence (Time of repetition (TR)/inversion time (TI)/echo time (TE) = 2400/1000/2.38 milliseconds, flip angle = 8°, and voxel size = 1 × 1 × 1 mm3, as described in our initial study (Heaps et al. 2012). Additional MRI sequences were obtained, including T2-weighted scans that were used primarily for the detection of white matter disease or other injury, but were not used in the processing of DWI images.

Axial diffusion-weighted images were acquired using a customized in-house single-shot multi-slice echo-planar pulse sequence. The tensor was encoded using 30 non-collinear diffusion-encoded directions that were repeated to provide 60 diffusion weighted volumes. All directions were acquired with a gradient weight of b = 1000s/mm^2. Six baseline acquisitions with a diffusion weighting of ~0 s/mm^2 were also obtained and interleaved with the diffusion weighted volumes. The following parameters were used: TE- 103 ms, TR 10 s, matrix 128 × 128, FOV 218 × 218 mm 70 contiguous isotropic

1.7 mm^3 voxels, full Fourier transform. Prior to image analysis, images were visually inspected and individuals who had evidence of white matter disease or visible lesions on T1 or T2 scans were excluded from further study participation.

Image analysis

Diffusion-weighted images (DWIs) were preprocessed using FSL 5.0 (Jenkinson et al. 2012). DWIs were corrected for motion and eddy-current induced artifacts through affine registration to the first baseline volume using FSL FLIRT (Jenkinson and Smith 2001) with the mutual information criteria. The orientations of the gradient encoding directions were corrected by the rotation induced by these registrations (Leemans and Jones 2009), and brain tissue was extracted using FSL brain extractions tool (BET) (Smith 2002) with a fraction threshold of 0.45. Diffusion tensor images were estimated for each subject using FSL DTIFIT.

Following this, a study-specific white matter atlas was created using DTI-TK (Zhang et al. 2007). The template diffusion tensor image was computed by iteratively deforming and averaging the population imaging data using the tensor-based deformable registration algorithm in DTI-TK (Zhang et al. 2006) with finite strain tensor reorientation and the deviatoric tensor similarity metric. This template was used to define inclusion and exclusion ROI masks for the anterior thalamic radiation (ATR), cingulum bundle (CING), the inferior frontal occipital fasciculus (IFOF), inferior longitudinal fasciculus (ILF), superior longitudinal fasciculus (SLF), and the uncinate fasciculus (UNC) (Mori and van Zijl 2002). Whole brain tractography was performed in the template image, and subsets of curves were interactively selected to represent each TOI. For each bundle, two inclusion TOI masks and one exclusion TOI mask were drawn in template space using ITK-SNAP (Yushkevich et al. 2006). The exclusion mask was used to remove erroneous stray fibers that can occur due to limitations such as noise and voxel size (Zhang et al. 2010). These masks were placed at opposite ends of each template tractography bundle, and drawn in reference to standard white matter atlases ((Catani and Thiebaut de Schotten 2012); (Oishi et al. 2009)).

Subject-specific fiber bundle metrics were computed as follows. First, the TOI inclusion and exclusion masks were deformed to subject native space using the DTI-TK registration. Whole brain tractography was then performed in subject native space and a subset of curves in the TOI was selected using the two inclusion and exclusion masks. Diffusion modeling for tractography used FSL XFIBRES to obtain ball-and-sticks diffusion models in each voxel (Behrens et al. 2007). Model fitting was performed with two stick compartments to improve tractography in areas with complex anatomy, such as crossing fibers. Tractography was performed using an extension of the standard streamline approach to use multiple fibers per voxels with the following parameters: four seeds per voxel, an angle threshold of 50°, a minimum length of 10 mm, and a minimum volume fraction of 0.1. During tracking, a kernel regression estimation framework (Cabeen et al. 2016) was used for smooth interpolation of the multi-fiber ball-and-sticks models with a Gaussian kernel with a spatial bandwidth of 1.5 mm and voxel neighborhood of $7\times7\times7$. Finally, the number of paths in each fiber bundle were calculated, then the average and sum FBL were computed from the distribution of streamline lengths in each bundle and retained for statistical analysis. Whole brain FBL-sum was calculated by summing the lengths of fiber bundles. Whole brain average FBL (FBL-avg) was calculated by averaging the lengths of fiber bundles. The FBL-avg of each TOI was calculated by computing the average length of all the fibers in the TOI. The FBL-sum of each TOI was calculated by summing the lengths of all the fibers in the TOI. Tracts of interest include: ATR, CING, IFOF, ILF, SLF, and UNC and were selected based on DTI findings in HIV (Hoare et al. 2011) as well as qtdMRI findings in other populations (Baker et al. 2014; Behrman-Lay et al. 2015; Bolzenius et al. 2013; Salminen et al. 2013). Intracranial volume was computed from the T_1-weighted MRI using Freesurfer version 5.1.0 (Fischl 2012).

Neuropsychological measures and depression screening

Neuropsychological methods are described in detail in Paul et al. (Paul et al. 2014). Briefly, a trained research technician fluent in Xhosa administered tests in the following domains: Learning/Memory, Executive Function, and Psychomotor speed (Table 1). HIV+ participants were screened for

Table 1 Neuropsychological measures

Learning/Memory	
Verbal	
	HVLT learning
	HVLT recall
Visual	
	BVMT learning
	BVMT recall
Executive Function	
	Color word interference
	Verbal fluency- animals
Working memory	
	Digit symbol
	Color trails 2
Visuoconstruction/Planning	
	Rey-O copy
	Block design
Processing speed	
	Trails A
	Color trails 1

HVLT Hopkins verbal learning test, *BVMT* Brief visual memory test

depression using either the Mini-International Neuropsychiatric Interview (M.I.N.I) (Sheehan et al. 1998) or total score on the Center for Epidemiologic Studies depression screen (CESD; (Radloff 1991). Individuals who screened positively for clinical depression were not included in the study.

Statistical analysis

Analyses were conducted with SPSS 23 (IBM; New York, NY). Primary analyses utilized Chi square tests and independent t-tests to examine demographic differences between groups on age, sex, and education (see Table 2). Additionally, we employed correlations between all of the FBL metrics, age, education, sex, and intracranial volume to determine the need for covariates in subsequent analyses. All variables were checked prior to analyses for normality of distributions. Holm's sequential Bonferroni was used to correct for multiple comparisons.

Whole brain FBL-avg and FBL-sum between HIV− and HIV+ were separately examined using univariate analyses (SPSS General Linear Model Univariate procedure). In each model, HIV status was the primary independent variable with age, sex, and intracranial volume entered as covariates and whole brain FBL-avg the dependent variable in the first analysis, and whole brain FBL-sum as the dependent variable in the second analysis. Separate multivariate linear models were used (SPSS General Linear Model Multivariate procedure) to test the effect of HIV status on the six TOIs. HIV status was the primary independent variable with age, gender, and intracranial volume included as covariates (ATR, CING, IFOF, ILF, SLF, and UNC). The FBL-avg values for each TOI were dependent variables i the first analysis, with FBL-sum TOIs as dependent variables in the second analysis. Post-hoc univariate analyses, adjusted for covariates, were used to determine which TOIs differed significantly between the groups. As a supplementary analysis, the effect of HIV status (with age, sex, and ICV as covariates) on the number of FBL paths in each TOI was examined using a multivariate model with the six TOIs as dependent variables. Spearman's correlations were completed to determine the degree of correspondence between the FBL metrics, duration of infection, current CD4 count, and viral load. CD4 cell count and viral load were natural log and log transformed, respectively, prior to analyses. Additional partial correlations controlling for age and intracranial volume were completed to inform the relationships between whole brain FBL metrics and the neuropsychological measures.

Results

Analysis of the demographic characteristics between the HIV+ and HIV− groups indicated significant group differences for age, sex, and education. The HIV+ group was older, on average ($m = 31.8$ years old, range 22–46) and had less education ($m = 10.3$ years) than the HIV− group ($m = 24.2$ years old, range 20–35, and $m = 11.1$ years of education). The HIV+ group was 81% female and the HIV− group was 52% female. All (100%) of the HIV+ group had a detectable viral load and 16.5% ($n = 27$) had initiated ART, with 6 of those individuals having received ART for less than 14 days. Education did not significantly correlate with any FBL measures (all $rs < 0.2$, $ps > 0.05$) and therefore we did not include education as a covariate in any of the analyses. Age, sex and intracranial volume were significantly correlated with several of the FBL measures and were therefore included as covariates in all of the FBL analyses.

HIV+ vs HIV− whole brain and tract-based FBL measures

Whole brain FBL-avg was similar between the two groups ($F_{(4,153)} = 1.91$, $p = 0.17$, $n^2 = 0.012$). In contrast, whole brain FBL-sum was significantly higher in the HIV− group (m = 9811.4) compared to the HIV+ group (m = 8028.3, $F_{(4, 153)} = 24.93$, $p < 0.001$, $n^2 = 0.14$, see Table 3).

The multivariate analysis for tract-based FBL-avg indicated a significant multivariate effect of HIV status (Wilks'

Table 2 Demographic information for the HIV+ and HIV− groups

	HIV+ $n = 135$		HIV− $n = 21$		
	Mean (SD)	Median (IQR)	Mean (SD)	Median (IQR)	$p=$
Age	31.81 (5.21)	31 (28–35.5)	24.24 (4.19)	24 (20–26)	0.0001
Education	10.26 (1.58)		11.14 (1.19)		0.015
Sex	81%		52%		0.0001
Current CD4	227	189 (115–315)			
LogVL $n = 124$	4.17	4.3 (3.4–4.87)			
% detectable VL	100%				
Duration of Infection $n = 111$	12.62				
Intracranial volume (ICV) cm^3	1292.6 (261.17)		1385.0 (246.70)		0.13

Table 3 Shows the mean average length of the whole brain metrics for the HIV+ and HIV− group after adjustment for age, sex, and intracranial volume. Only the whole brain FBL sum metric was significantly different between the HIV+ and the HIV− group

Univariate analysis of whole brain FBL metrics				
Group	Mean	Std. Error	95% Confidence interval	
			Lower bound	Upper bound
FBL average				
HIV−	61.1	0.62	59.87	62.33
HIV+	60.16	0.22	59.72	60.59
FBL sum				
HIV−	9,811,456.1	327,035.04	9,165,368.86	10,457,543.4
HIV+	8,028,280.8	115,356.43	7,800,383.75	8,256,177.85

Covariates were evaluated at the following values: sex = 0.23, participant_age = 30.85, intracranialvol = 1,304,894.91 mm^3

Lambda = 0.876, $F_{(6, 146)} = 3.45$, $p = 0.003$, $n^2 = 0.12$) with the HIV+ group exhibiting significantly shorter FBL-avg compared to the HIV− group. In post-hoc univariate comparisons, HIV+ individuals exhibited shorter FBL-avg in the ILF ($p < 0.01$) and ATR ($p < 0.01$) after multiple comparison corrections (Holm-Bonferroni; (Holm 1979). The multivariate model for tract-based FBL-sum revealed a significant multivariate effect of HIV on FBL-sum (Wilks' Lambda = 0.875, $F_{(6, 146)} = 3.462$, $p = 0.003$, $n^2 = 0.13$, see Table 4). All six tracts for FBL-sum were significantly less in the HIV+ group compared to the HIV− group in each TOI (Table 4). A visualization of the tracts in a representative HIV+ subject compared to the template is provided in Fig. 1.

As a supplementary analysis, we examined the number of FB paths for the TOIs using the same multivariate model describe above with HIV status as the primary independent variable and age, gender, and intracranial volume as covariates. The HIV+ group had fewer FB paths in all of the TOI, with significant group differences noted in four of the six tracts (CING, IFOF, SLF, UNC) compared to the HIV− group (see supplementary table 1). In a follow-up analysis, the whole brain and TOI analyses were repeated with the 27 individuals who had initiated ART removed from the HIV+ group leaving 108 HIV+ participants in the analysis. The pattern of results remained the same, with the HIV+ group having shorter FBL-sum, and shorter TOI in 4 of the 6 tracts examined (see supplementary table 2 for details).

Correlations between FBL metrics, disease burden, inflammatory markers, and neuropsychological performance

Neither CD4 count, nor time since diagnosis, nor viral load correlated with any of the FBL metrics. Whole brain FBL

Table 4 Shows the mean values for each TOI for the FBL mean and FBL sum analyses

TOI	HIV+				HIV−				
			95% CI				95% CI		
	Mean	SE	Lower	Upper	Mean	SE	Lower	Upper	p
FBL average									
ATR	158.0	0.7	156.6	159.4	164.1	2.0	160.2	168.0	0.005*
IFOF	273.2	1.3	270.7	275.7	280.8	3.6	273.7	287.8	0.056
ILF	184.3	1.1	182.2	186.4	198.1	3.1	192.0	204.1	< 0.001*
SLF	112.9	0.9	111.0	114.7	115.6	2.6	110.4	120.8	0.341
CING	157.3	1.5	154.4	160.2	167.1	4.1	159.0	175.3	0.031*
UNC	127.8	1.5	124.9	130.7	139.1	4.1	130.9	147.2	0.013*
FBL sum									
ATR	116.2	4.2	107.9	124.5	143.1	11.8	119.8	166.6	0.039*
IFOF	460.2	14.0	430.7	489.7	613.7	42.0	530.7	696.8	0.001*
ILF	284.3	9.3	265.8	302.8	349.6	26.4	297.5	401.6	0.021*
SLF	955.9	3.0	896.5	101.5	121.5	8.5	104.8	138.3	0.006*
CING	118.0	4.0	110.1	125.9	148.3	11.3	126.0	170.5	0.015*
UNC	38.4	2.0	34.4	42.4	55.1	5.7	43.8	66.3	0.008*

Covariates were evaluated at the following values: sex = 0.23, participant_age = 30.85, intracranialvol = 1306322.86

CI confidence interval, *SE* standard error, *TOI* tract of interest, *ATR* anterior thalamic radiation

IFOF inferior fronto-occipical fasciculus, *ILF* inferior longitudinal fasciculus, *SLF* superior longitudinal fasciculus, *CING* cingulum bundle, *UNC* uncinate fasciculus

All values for FBL-sum have been adjusted by 10^-3 to reduce significant figures

* indicates TOI significantly different between groups after correction for multiple comparisons (Holm-Sidak)

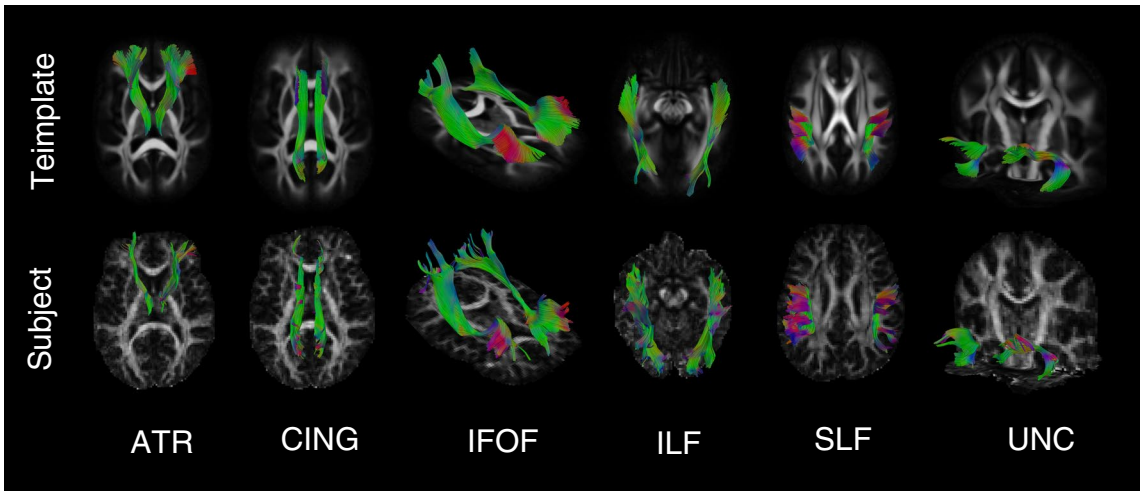

Fig. 1 Shows each of the tracts of interest examined in the study. The template images on top depict the templates used to determine inclusion and exclusion masks for each tract of interest. The subject images on the bottom depict the tractography of an HIV-postitive participant's tracts of interest. *ATR* anterior thalamic radiation, *CING* cingulum bundle, *IFOF* inferior frontal occipital fasiculus, *ILF* inferior longitudinal fasiculus, *SLF* superior longitudinal fasiculus, *UNC* uncinate fasciculus

metrics were modestly correlated with neuropsychological performance with the most robust covariance between FBL-sum and spatial learning and memory (Table 5). These correlations were repeated, excluding the 27 individuals who had initiated ART removed from the HIV+ group leaving 108 HIV+ individuals and 21 HIV− in the analysis. With the HIV+ individuals on ART removed from the analysis the relationship between the whole brain FBL metrics and neuropsychological measures changed such that visual learning was no longer significantly associated with whole brain FBL-sum. Results are detailed in Supplementary table 3.

Discussion

This study extends the current literature examining the effect of HIV on white matter microstructure by examining the whole brain and TOI abnormalities in HIV-C. Differences were evident in whole brain FBL-sum, but not whole brain FBL-avg. Tract-specific FBL differences were also examined between the HIV+ and HIV− groups in six tracts of interest. Our results provide the first *in vivo* evidence of shorter FBL-sum in the ILF, SLF, ATR, IFOF, CING and UNC in HIV+ individuals. Additionally, there was an effect of HIV on the FBL-avg metric in the TOI, with the IFOF, ILF, CING and ATR tracts significantly shorter in the HIV+ group. Whole brain FBL metrics were modestly associated with neuropsychological performance, with higher FBL-sum corresponding with better performance. None of the FBL metrics were associated with markers of disease burden such as CD4 cell count, viral load, or duration of infection. These results provide seminal evidence of reduced sum of FBL in HIV whole brain and TOI, with shorter average FBL in select TOI.

FBL provides unique characterizations of white matter fibers that are meant to represent the biological lengths of fiber bundles. Shorter average FBL theoretically reflect a shorter average length of all the fibers within a bundle, or group of axons. Similarly, FBL-sum reflects the summed length of all the fibers within a bundle. Smaller FBL-sum may reflect a combination of both shortening of the fibers and/or fewer fibers within the bundle resulting from factors, such as inflammation and viral toxicity, that promote neuronal degradation (Scaravilli et al. 2007). The whole brain FBL metrics each provide unique information about the architecture of white matter fiber bundles in the brain. However, unlike biological bundle length, FBL is also likely to be sensitive to microstructural changes within bundles, to some extent, for example, when changes to the microstructure are sufficiently abnormal to change the course of tractography constructions. In the current analysis, mean differences in FBL were not observed in the whole brain measures; however, HIV+ individuals exhibited shorter FBL-avg in the

Table 5 Shows the values of the partial correlations between the whole brain qtdMRI metrics and neuropsychological measures controlling for age and intracranial volume. Measures that did not have a significant relationship with the qtdMRI metrics were not included in the table

	Whole Brain FBL sum
BVMT learn	0.32**
BVMT recall	0.31**
WCST per errors	−0.20*
Digit symbol	0.15*
Verbal fluency	0.21**
Block design	0.20**

BVMT Brief Visual Memory Test, *WCST* Wisconsin Card Sort Test

*$p < 0.05$; **$p < 0.01$

ILF, and the ATR. FBL-sum was reduced in all six TOI, and our supplementary analysis of number of FBL confirmed that there were significantly fewer fiber bundles in the ATR, CING, IFOF, and UNC. Taken together, our findings suggest that HIV neuropathogenesis in HIV-C initially involves reductions in the number of white matter fibers to a greater extent than average tract length. It is also possible that the changes along a fiber bundle take place at earlier stages of disease, and ultimately result in the reduced number of fibers, resulting in smaller FBL-sum values. Future work can help to better understand these factors by examining the relation between FBL and microstructural properties such as fiber orientation dispersion and neurite density.

Reductions in FBL-avg and FBL-sum likely result from immune activation evident in untreated HIV and downstream effects on anisotropic diffusion of water along fiber bundles or myelin (Beaulieu 2002). Studies have associated abnormalities in DTI metrics within specific tracts to cognitive deficits in the domains of processing speed, working memory, and executive functions (Biesbroek et al. 2013) as well as affective states, including apathy (Zappala et al. 2012). Deficits in these cognitive domains are commonly reported in HIV (Heaton et al. 2010); (Paul et al. 2005; Tate et al. 2003). The results of this study show an association between shorter whole brain FBL sum and poorer performance on measures of learning, memory, visuoconstruction, verbal fluency and executive function. However, the strength of the relationships is limited, and the cross-sectional nature of this study does not inform long-term outcomes after sustained ART with viral suppression. Since the results of this study indicate that reduced FBL sum is associated with poorer neuropsychological performance there is an indication that this is due to fewer FBL, as opposed to shorter fiber bundle length due to the lack of correlation between FBL average and the neuropsychological measures. It is also possible that adequate connections have atrophied, or become "disconnected" resulting in poorer neuropsychological performance.

One longitudinal study of DTI in HIV reported significant changes in diffusion metrics indicating progressive white matter and cognitive decline in an ART stable HIV+ group after one year (Chang et al. 2008). Conversely, a recent longitudinal study of HIV+ individuals on stable highly-active ART did not find changes to DTI scalar metrics after approximately 26 months, but cognitive function was not assessed (Correa et al. 2016). Additional studies will be critical to better understand whether there is potential for recovery of FBL through therapeutic interventions, and how FBL changes affect cognition and daily living functions.

There are several limitations to our study that warrant discussion. This study involved a cross-sectional design and as such we cannot determine the progression of FBL changes over time. Longitudinal studies will be key to understanding how FBL can change across time, with ART or other conjunctive therapies to protect the brain. A number of individuals in this study had recently initiated ART therapy (within 30 days of their MRI), which may impact the degree of correspondence between markers of CD4 and viral load to FBL. A relatively small number of HIV− controls were available for the study; however, there was sufficient power to detect strong differences between groups using FBL as a measure of white matter integrity. Untreated HIV has been associated with the development of white matter disease, and our exclusion of individuals with overt white matter disease may not be fully representative of individuals with untreated HIV. As indicated in our supplementary analysis, it is possible that ART initiation in the small percentage of participants in the study influenced the relationship between cognitive performance and FBL-sum TOI metrics. However, duration of treatment was under 30 days and all of the participants had detectable viral loads. Therefore, it is unlikely that ART initiation in this subset significantly affected the outcomes.

Our results confirm abnormalities in FBL-sum in whole brain and TOI among HIV+ individuals ART in South Africa. These abnormalities indicate that long-range fiber bundles connecting the frontal lobe to each the temporal, parietal, and occipital lobes have shorter summed FBL, on average, than HIV− individuals. Additionally, the results suggest global measurements of FBL-sum may be more powerful to detect white matter abnormalities in HIV than FBL-avg. Shorter sum of FBL indicates either reduced FBL fiber volume, or fibers that have shortened along the anatomical tract. However, a significant whole brain difference in FBL-avg was not evident; therefore, it is likely that a reduction in the number of fibers are driving the FBL-sum metric lower in HIV, and not shortening of fibers along a path. Given that the study population was naïve to ART or had newly initiated ART future work will be critical to understanding how stable treatment with ART may affect FBL metrics and neuropsychological performance. This study provides a snapshot of white matter integrity, and future studies following individuals over time are necessary to understand the trajectory of brain health using qtdMRI and potential legacy effects of ART in HIV. Furthermore, there are a number of host and viral factors (e.g. resilience, inflammatory markers, and HIV co-receptor tropism) that may affect how FBL change in HIV that remain to be examined.

Compliance with ethical standards

Funding Funding for this study was provided by the National Institute of Mental Health to Robert H. Paul R01MH085604.

Conflict of interest Authors have no conflicts of interest to declare.

Ethical approval All procedures were approved by the institutional review boards for human subjects' research at the University of Missouri-

St. Louis and the University of Cape Town in accordance with the ethical standards national research committee and with the 1964 Helsinki declaration and its later amendments or comparable ethical standards.

Informed consent Informed consent was obtained from all individual participants included in the study.

References

Alexander, A. L., et al. (2011). Characterization of cerebral white matter properties using quantitative magnetic resonance imaging stains. *Brain Connectivity, 1*(6), 432–446. https://doi.org/10.1089/brain.2011.0071.

Ances, B. M., & Hammoud, D. A. (2014). Neuroimaging of HIV associated neurocognitive disorders (HAND). *Current Opinion in HIV and AIDS, 9*(6), 545.

Baker, L. M., Cooley, S. A., Cabeen, R. P., Laidlaw, D. H., Joska, J. A., Hoare, J., et al. (2017). Topological organization of whole-brain white matter in HIV infection. *Brain Connectivity, 7*(2), 115–122. https://doi.org/10.1089/brain.2016.0457.

Baker, L. M., Laidlaw, D. H., Cabeen, R., Akbudak, E., Conturo, T. E., Correia, S., et al. (2016). Cognitive reserve moderates the relationship between neuropsychological performance and white matter fiber bundle length in healthy older adults. *Brain Imaging and Behavior*. https://doi.org/10.1007/s11682-016-9540-7.

Baker, L. M., Laidlaw, D. H., Conturo, T. E., Hogan, J., Zhao, Y., Luo, X., et al. (2014). White matter changes with age utilizing quantitative diffusion MRI. *Neurology, 83*(3), 247–252. https://doi.org/10.1212/WNL.0000000000000597.

Beaulieu, C. (2002). The basis of anisotropic water diffusion in the nervous system - a technical review. *NMR in Biomedicine, 15*(7–8), 435–455. https://doi.org/10.1002/nbm.782.

Behrens, T. E., Berg, H. J., Jbabdi, S., Rushworth, M. F., & Woolrich, M. W. (2007). Probabilistic diffusion tractography with multiple fibre orientations: what can we gain? *NeuroImage, 34*(1), 144–155. https://doi.org/10.1016/j.neuroimage.2006.09.018.

Behrman-Lay, A. M., Usher, C., Conturo, T. E., Correia, S., Laidlaw, D. H., Lane, E. M., et al. (2015). Fiber bundle length and cognition: a length-based tractography MRI study. *Brain Imaging and Behavior, 9*(4), 765–775. https://doi.org/10.1007/s11682-014-9334-8.

Biesbroek, J. M., Kuijf, H. J., van der Graaf, Y., Vincken, K. L., Postma, A., Mali, W. P., et al. (2013). Association between subcortical vascular lesion location and cognition: a voxel-based and tract-based lesion-symptom mapping study. The SMART-MR study. *PLoS One, 8*(4), e60541. https://doi.org/10.1371/journal.pone.0060541.

Bolzenius, J. D., Laidlaw, D. H., Cabeen, R. P., Conturo, T. E., McMichael, A. R., Lane, E. M., et al. (2013). Impact of body mass index on neuronal fiber bundle lengths among healthy older adults. *Brain Imaging and Behavior, 7*(3), 300–306. https://doi.org/10.1007/s11682-013-9230-7.

Bolzenius, J. D., Laidlaw, D. H., Cabeen, R. P., Conturo, T. E., McMichael, A. R., Lane, E. M., et al. (2015). Brain structure and cognitive correlates of body mass index in healthy older adults. *Behavioural Brain Research, 278*, 342–347. https://doi.org/10.1016/j.bbr.2014.10.010.

Buch, S., Chivero, E. T., Hoare, J., Jumare, J., Nakasujja, N., Mudenda, V., et al. (2016). Proceedings from the NIMH symposium on "NeuroAIDS in Africa: neurological and neuropsychiatric complications of HIV". *Journal of Neurovirology, 22*(5), 699–702.

Cabeen, R. P., Bastin, M. E., & Laidlaw, D. H. (2016). Kernel regression estimation of fiber orientation mixtures in diffusion MRI. *NeuroImage, 127*, 158–172. https://doi.org/10.1016/j.neuroimage.2015.11.061.

Catani, M., & Thiebaut de Schotten, M. (2012). *Atlas of human brain connections*. Oxford, Oxford University Press.

Chang, L., Wong, V., Nakama, H., Watters, M., Ramones, D., Miller, E. N., et al. (2008). Greater than age-related changes in brain diffusion of HIV patients after 1 year. *Journal of Neuroimmune Pharmacology, 3*(4), 265–274. https://doi.org/10.1007/s11481-008-9120-8.

Correa, D. G., Zimmermann, N., Tukamoto, G., Doring, T., Ventura, N., Leite, S. C., et al. (2016). Longitudinal assessment of subcortical gray matter volume, cortical thickness, and white matter integrity in HIV-positive patients. *Journal of Magnetic Resonance Imaging*. https://doi.org/10.1002/jmri.25263.

Correia, S., Lee, S. Y., Voorn, T., Tate, D. F., Paul, R. H., Zhang, S., et al. (2008). Quantitative tractography metrics of white matter integrity in diffusion-tensor MRI. *NeuroImage, 42*(2), 568–581. https://doi.org/10.1016/j.neuroimage.2008.05.022.

de Almeida, S. M., Ribeiro, C. E., de Pereira, A. P., Badiee, J., Cherner, M., Smith, D., et al. (2013). Neurocognitive impairment in HIV-1 clade C- versus B-infected individuals in Southern Brazil. *Journal of Neurovirology, 19*(6), 550–556. https://doi.org/10.1007/s13365-013-0215-5.

Fischl, B. (2012). FreeSurfer. *NeuroImage, 62*(2), 774–781. https://doi.org/10.1016/j.neuroimage.2012.01.021.

Heaps, J. M., Joska, J., Hoare, J., Ortega, M., Agrawal, A., Seedat, S., et al. (2012). Neuroimaging markers of human immunodeficiency virus infection in South Africa. *Journal of Neurovirology, 18*(3), 151–156. https://doi.org/10.1007/s13365-012-0090-5.

Heaton, R. K., Clifford, D. B., Franklin, D. R. Jr., Woods, S. P., Ake, C., Vaida, F., et al. (2010). HIV-associated neurocognitive disorders persist in the era of potent antiretroviral therapy: CHARTER study. *Neurology, 75*(23), 2087–2096. https://doi.org/10.1212/WNL.0b013e318200d727.

Hoare, J., Fouche, J. P., Phillips, N., Joska, J. A., Donald, K. A., Thomas, K., & Stein, D. J. (2015). Clinical associations of white matter damage in cART-treated HIV-positive children in South Africa. *Journal of Neurovirology, 21*(2), 120–128. https://doi.org/10.1007/s13365-014-0311-1.

Hoare, J., Fouche, J. P., Spottiswoode, B., Joska, J. A., Schoeman, R., Stein, D. J., & Carey, P. D. (2010). White matter correlates of apathy in HIV-positive subjects: a diffusion tensor imaging study. *The Journal of Neuropsychiatry and Clinical Neurosciences, 22*(3), 313–320. https://doi.org/10.1176/appi.neuropsych.22.3.313. https://doi.org/10.1176/jnp.2010.22.3.313.

Hoare, J., Fouche, J. P., Spottiswoode, B., Sorsdahl, K., Combrinck, M., Stein, D. J., et al. (2011). White-matter damage in clade C HIV-positive subjects: a diffusion tensor imaging study. *The Journal of Neuropsychiatry and Clinical Neurosciences, 23*(3), 308–315. https://doi.org/10.1176/appi.neuropsych.23.3.308. https://doi.org/10.1176/jnp.23.3.jnp308.

Hoare, J., Westgarth-Taylor, J., Fouche, J. P., Combrinck, M., Spottiswoode, B., Stein, D. J., & Joska, J. A. (2013). Relationship between apolipoprotein E4 genotype and white matter integrity in HIV-positive young adults in South Africa. *European Archives of Psychiatry and Clinical Neuroscience, 263*(3), 189–195. https://doi.org/10.1007/s00406-012-0341-8.

Hoare, J., Westgarth-Taylor, J., Fouche, J. P., Spottiswoode, B., Paul, R., Thomas, K., et al. (2012). A diffusion tensor imaging and neuropsychological study of prospective memory impairment in South African HIV positive individuals. *Metabolic Brain Disease, 27*(3), 289–297. https://doi.org/10.1007/s11011-012-9311-0.

Holm, S. (1979). A simple sequentially rejective multiple test procedure. *Scandinavian Journal of Statistics, 6*(2), 65–70.

Jenkinson, M., Beckmann, C. F., Behrens, T. E., Woolrich, M. W., & Smith, S. M. (2012). Fsl. *Neuroimage, 62*(2), 782–790. https://doi.org/10.1016/j.neuroimage.2011.09.015.

Jenkinson, M., & Smith, S. (2001). A global optimisation method for robust affine registration of brain images. *Medical Image Analysis, 5*(2), 143–156.

Joska, J. A., Fincham, D. S., Stein, D. J., Paul, R. H., & Seedat, S. (2010). Clinical correlates of HIV-associated neurocognitive disorders in South Africa. *AIDS and Behavior, 14*(2), 371–378. https://doi.org/10.1007/s10461-009-9538-x.

Joska, J. A., Westgarth-Taylor, J., Hoare, J., Thomas, K. G., Paul, R., Myer, L., & Stein, D. J. (2012). Neuropsychological outcomes in adults commencing highly active anti-retroviral treatment in South Africa: a prospective study. *BMC Infectious Diseases, 12*, 39. https://doi.org/10.1186/1471-2334-12-39.

Joska, J. A., Westgarth-Taylor, J., Myer, L., Hoare, J., Thomas, K. G., Combrinck, M., et al. (2011). Characterization of HIV-associated neurocognitive disorders among individuals starting antiretroviral therapy in South Africa. *AIDS and Behavior, 15*(6), 1197–1203. https://doi.org/10.1007/s10461-010-9744-6.

Leemans, A., & Jones, D. K. (2009). The B-matrix must be rotated when correcting for subject motion in DTI data. *Magnetic Resonance in Medicine, 61*(6), 1336–1349. https://doi.org/10.1002/mrm.21890.

Masters, M. C., & Ances, B. M. (2014). Role of neuroimaging in HIV-associated neurocognitive disorders. In *Seminars in neurology* (Vol. 34, No. 01, pp. 89–102). New York: Thieme Medical Publishers.

Mori, S., & van Zijl, P. C. (2002). Fiber tracking: principles and strategies - a technical review. *NMR in Biomedicine, 15*(7–8), 468–480. https://doi.org/10.1002/nbm.781.

Nath, A. (2015). Eradication of human immunodeficiency virus from brain reservoirs. *Journal of Neurovirology, 21*(3), 227–234.

Oishi, K., Faria, A., Jiang, H., Li, X., Akhter, K., Zhang, J., et al. (2009). Atlas-based whole brain white matter analysis using large deformation diffeomorphic metric mapping: application to normal elderly and Alzheimer's disease participants. *NeuroImage, 46*(2), 486–499.

Ortega, M., Heaps, J. M., Joska, J., Vaida, F., Seedat, S., Stein, D. J., et al. (2013). HIV clades B and C are associated with reduced brain volumetrics. *Journal of Neurovirology, 19*(5), 479–487. https://doi.org/10.1007/s13365-013-0202-x.

Paul, R. H., Brickman, A. M., Navia, B., Hinkin, C., Malloy, P. F., Jefferson, A. L., et al. (2005). Apathy is associated with volume of the nucleus accumbens in patients infected with HIV. *The Journal of Neuropsychiatry and Clinical Neurosciences, 17*(2), 167–171. https://doi.org/10.1176/jnp.17.2.167.

Paul, R. H., Joska, J. A., Woods, C., Seedat, S., Engelbrecht, S., Hoare, J., et al. (2014). Impact of the HIV Tat C30C31S dicysteine substitution on neuropsychological function in patients with clade C disease. *Journal of Neurovirology, 20*(6), 627–635. https://doi.org/10.1007/s13365-014-0293-z.

Paul, R. H., Phillips, S., Hoare, J., Laidlaw, D. H., Cabeen, R., Olbricht, G. R., et al. (2017). Neuroimaging abnormalities in clade C HIV are independent of Tat genetic diversity. *Journal of Neurovirology, 23*(2), 319–328. https://doi.org/10.1007/s13365-016-0503-y.

Radloff, L. S. (1991). The use of the center for epidemiologic studies depression scale in adolescents and young adults. *Journal of Youth and Adolescence, 20*(2), 149–166. https://doi.org/10.1007/BF01537606.

Ragin, A. B., Wu, Y., Gao, Y., Keating, S., Du, H., Sammet, C., et al. (2015). Brain alterations within the first 100 days of HIV infection. *Annals of Clinical and Translational Neurology, 2*(1), 12–21.

Salminen, L. E., Schofield, P. R., Lane, E. M., Heaps, J. M., Pierce, K. D., Cabeen, R., et al. (2013). Neuronal fiber bundle lengths in healthy adult carriers of the ApoE4 allele: a quantitative tractography DTI study. *Brain Imaging and Behavior, 7*(3), 274–281. https://doi.org/10.1007/s11682-013-9225-4.

Scaravilli, F., Bazille, C., & Gray, F. (2007). Neuropathologic contributions to understanding AIDS and the central nervous system. *Brain Pathology, 17*(2), 197–208. https://doi.org/10.1111/j.1750-3639.2007.00047.x.

Sheehan, D. V., Lecrubier, Y., Sheehan, K. H., Amorim, P., Janavs, J., Weiller, E., et al. (1998). The Mini-International Neuropsychiatric Interview (M.I.N.I.): the development and validation of a structured diagnostic psychiatric interview for DSM-IV and ICD-10. *The Journal of Clinical Psychiatry, 59*(Suppl 20), 22–33; quiz 34–57.

Seider, T. R., Gongvatana, A., Woods, A. J., Chen, H., Porges, E. C., Cummings, T., et al. (2016). Age exacerbates HIV-associated white matter abnormalities. *Journal of Neurovirology, 22*(2), 201–212.

Smith, S. M. (2002). Fast robust automated brain extraction. *Human Brain Mapping, 17*(3), 143–155. https://doi.org/10.1002/hbm.10062.

Tate, D., Paul, R. H., Flanigan, T. P., Tashima, K., Nash, J., Adair, C., et al. (2003). The impact of apathy and depression on quality of life in patients infected with HIV. *AIDS Patient Care and STDs, 17*(3), 115–120. https://doi.org/10.1089/108729103763807936.

Tate, D. F., Conley, J., Paul, R. H., Coop, K., Zhang, S., Zhou, W., et al. (2010). Quantitative diffusion tensor imaging tractography metrics are associated with cognitive performance among HIV-infected patients. *Brain Imaging and Behavior, 4*(1), 68–79. https://doi.org/10.1007/s11682-009-9086-z.

Thompson, P. M., & Jahanshad, N. (2015). Novel neuroimaging methods to understand how HIV affects the brain. *Current HIV/AIDS Reports, 12*(2), 289–298.

Wright, P., Heaps, J., Shimony, J. S., Thomas, J. B., & Ances, B. M. (2012). The effects of HIV and combination antiretroviral therapy on white matter integrity. *AIDS (London, England), 26*(12), 1501.

Yushkevich, P. A., Piven, J., Hazlett, H. C., Smith, R. G., Ho, S., Gee, J. C., & Gerig, G. (2006). User-guided 3D active contour segmentation of anatomical structures: significantly improved efficiency and reliability. *NeuroImage, 31*(3), 1116–1128. https://doi.org/10.1016/j.neuroimage.2006.01.015.

Zappala, G., Thiebaut de Schotten, M., & Eslinger, P. J. (2012). Traumatic brain injury and the frontal lobes: what can we gain with diffusion tensor imaging? *Cortex, 48*(2), 156–165. https://doi.org/10.1016/j.cortex.2011.06.020.

Zhang, H., Yushkevich, P. A., Alexander, D. C., & Gee, J. C. (2006). Deformable registration of diffusion tensor MR images with explicit orientation optimization. *Medical Image Analysis, 10*(5), 764–785. https://doi.org/10.1016/j.media.2006.06.004.

Zhang, H., Avants, B. B., Yushkevich, P. A., Woo, J. H., Wang, S., McCluskey, L. F., et al. (2007). High-dimensional spatial normalization of diffusion tensor images improves the detection of white matter differences: an example study using amyotrophic lateral sclerosis. *IEEE Transactions on Medical Imaging, 26*(11), 1585–1597. https://doi.org/10.1109/TMI.2007.906784.

Zhang, H., Awate, S. P., Das, S. R., Woo, J. H., Melhem, E. R., Gee, J. C., & Yushkevich, P. A. (2010). A tract-specific framework for white matter morphometry combining macroscopic and microscopic tract features. *Medical Image Analysis, 14*(5), 666–673.